Identification of boiling nucleation sites by non-orthogonal empirical functions (NEF) analysis of thermographic data

J. von Hardenberg (a), T. Kono (b), D.B.R.Kenning (b)
P.E. McSharry (a,b), L.A.Smith (a)
Oxford University
(a) Mathematical Institute, Oxford OX1 3LB,
(b) Department of Engineering Science, Oxford OX1 3PJ, United Kingdom

Abstract

The new method of analysis by non-orthogonal empirical functions (NEFs) is applied to experimental data for the spatio-temporal variations in wall temperature during nucleate boiling. It is shown that the method can successfully identify the positions and patterns of activity at individual members of a large group of nucleation sites. Statistical methods are developed for comparing data of this sort with numerical simulations.

1. Introduction

The transfer of heat by nucleate boiling is inherently non-uniform in time and space. The fluctuations in local conditions modify the activity of bubble nucleation sites in ways that cannot be represented by a simple relationship between space-time averaged wall superheat and the effective size distribution of the nucleation sites. The interactions between large groups of sites can be simulated by numerical models at low heat flux (e.g. Pasamehmetoglu and Nelson 1991, Unal and Pasamehmetoglu 1994, Golobic et al.,1996), and at high heat flux (e.g. Sadasivan et al. 1995, He et al., 2001), with approximate representations of events in the fluid phases. For the special conditions of boiling on a very thin, electrically-heated plate, the variations in temperature on the back of the plate can be measured experimentally by liquid crystal thermography, with simultaneous high-speed video recording of the bubble activity, (Kenning and Yan, 1996). Comparisons between models and experiments over short periods and small regions suggest improvements to the physics incorporated in the numerical models. Comparisons over long periods for systems comprising many nucleation sites require efficient computerised processing of large spatio-temporal data files and, because of the nonlinear dynamics of boiling, the development of appropriate statistical criteria. This paper describes continuing investigations of these issues.

Experiments on pool boiling of water at atmospheric pressure on a horizontal, electrically-heated plate of stainless steel 42 mm x 20 mm x 0.13 mm thick were described by Kenning and Yan (1996). The colourplay of a thin layer of liquid crystal on the bottom of the plate and the bubble activity on the top were recorded in the same colour video field at 200 interlaced fields/s. Separated Hue fields were converted to temperature fields by a pre-stored calibration and Intensity fields were used for the identification and measurement of bubbles. The growth of each bubble caused rapid local cooling over the near-circular contact area between the bubble and the wall; the wall temperature had to recover before the next bubble could nucleate. This cycle was interrupted if the cooled area of one site overlapped another site. At a heat flux of 51 kW/m^2, 48 sites in a central area 20 mm x 11 mm that produced bubbles during a period of 12 seconds were identified by manual analysis of the simultaneous recordings of temperature and bubble motion. Sites were identified by tracing a circular cooled patch back in time to the instant of its first appearance. The bubble view was then checked to confirm the first appearance of a bubble. The interactions between four adjacent sites were studied in detail over the same period. The manual analysis required weeks of work, making it impractical to study interactions over a longer period. McSharry et al. (2000) applied nonlinear analysis to the temperature-time series at the known positions of the four sites over a period of 30 seconds. They used a simple set of rules to identify bubble nucleation events and obtained statistical evidence for site interactions without reference to the bubble recordings. They showed that the previous analysis over a shorter period gave an inaccurate representation of the pattern of interaction over the longer period.

The bubble side cannot always be observed clearly at higher heat fluxes and in other boiling geometries so it is desirable to deduce the positions and activity of nucleation sites from the temperature data alone over periods of at least 30 seconds, by fully automated analysis. A conventional approach to such problems is principal

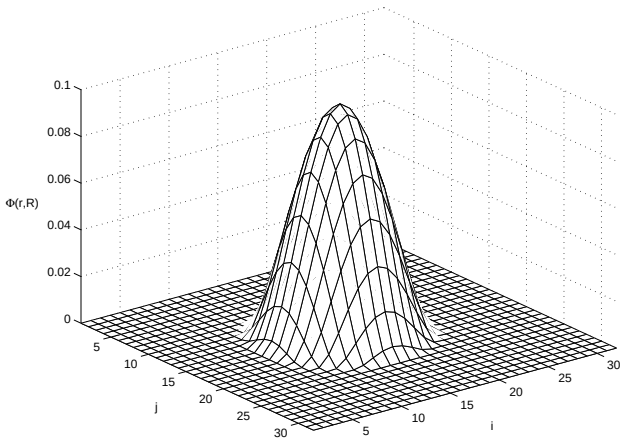

Figure 1: Typical NEF basis function.

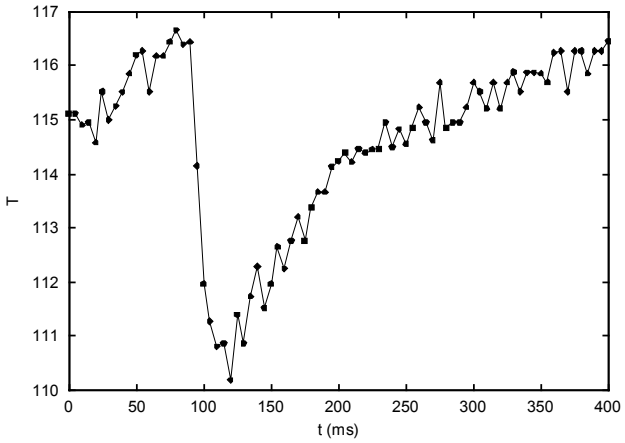

Figure 2: Evolution in time of temperature at the center of a cooling region during a nucleation.event.

component analysis by empirical orthogonal functions (EOFs). McSharry et al. (2001) showed that nucleation sites could be identified much more efficiently by a new method employing non-orthogonal empirical functions (NEFs) of a radially symmetric shape suggested by the physics of the cooling process during bubble growth, such as in Figure 1. The original temperature field is represented by a linear combination of NEFs of different positive or negative amplitude and radial scale, so as to minimise the variance between the original and reconstructed fields. In principle, a reconstruction to any desired degree of accuracy can be achieved by using sufficient NEFs; minimization of an appropriate cost function is used to balance the reconstruction error against the number of NEFs employed. The advantage of using NEFs with a physically based, realistic shape is that only a small number is needed to obtain a sufficiently accurate reconstruction and the properties of the NEFs can be interpreted physically. McSharry et al. described the implementation of this new method and applied it to a small area 5 mm x 5 mm containing only a few bubble nucleation sites, which were identified by the centres of the negative (i.e. cooling) NEFs occurring most frequently in the set of individual fields. Use of the additional information obtainable from temporal correlations was explored only in a preliminary way.

In this paper the NEF analysis is applied successfully to detect the much larger number of sites active over 30 s in the area 20 mm x 11 mm examined by Kenning and Yan (1996). Short-term temporal correlations are used to distinguish nucleation events from NEFs caused by other cooling processes. Following detection of each event, its position and timing, the local wall superheat immediately before the event and the size and amplitude of the NEFs immediately after the event are recorded for analysis by a variety of methods. Practical aspects of the NEF method are discussed in Section 2. Examples of preliminary results of the analysis are presented in Section 3.

2. Practical aspects of NEF analysis

2.2. General aspects of the data analysis

Hue data for a selected wall region 20 mm x 11 mm, were converted to temperatures in an array of 203 columns x 64 rows, the distance between columns being Δ_x=0.099 mm and between rows Δ_y=0.172 mm. The time interval between arrays was 5 ms. A sequence of 6 x 10^3 arrays was analysed. The interlacing of video fields leads to a small alternating vertical displacement of pixel rows, which is here ignored. McSharry et al. (2001) averaged successive interlaced frames, reducing the resolution in time.

The measured temperature fields present a strong constant spatial inhomogeneity, presumably due to boundary effects, large scale convective motion in the fluid and possible inhomogeneity in the characteristics of the liquid crystal. When considering data frames one at a time, it is impossible to distinguish these constant features from temporary cooled regions due to the formation of bubbles. In order to avoid this problem, similarly to the previous

manual study (Kenning and Yan, 1996), we choose to study the first difference in time between successive fields. This has the advantage of removing the constant spatial inhomogeneities, but can lead to increased sensitivity to noise. A 3 x 3 spatial averaging filter is used to reduce noise in the derived dataset.

NEF analysis has a few free parameters: First the shape of prototypical NEFs must be chosen, possibly based on the physics of the problem under study. In order to account for the different horizontal and vertical resolutions, since NEFs are applied directly to the data arrays, we use a modified ellipsoidal shape, based on the shape described in McSharry et al. (2001) and illustrated in Figure 1, with an aspect ratio (vertical over horizontal radius) of Δ_x / Δ_y. This is equivalent to a circular shape in physical coordinates. We allowed only negative amplitude NEFs to be used in the analysis. A realistic range of radii in the interval 6-36Δ_y is explored, allowing only for even multiples of Δ_y, in order to reduce the computational time needed for the analysis. The other important free parameter of NEF analysis is the tuning of the cost function (described in McSharry et al.), expressed by a penalty weighting factor α which affects the number of NEFs used for the reconstruction. A too low choice of this parameter leads to the detection of spurious NEFs associated with random background fluctuations or to more than one NEF being used to represent strongly deformed, non-circular, cooled regions. A too high value prevents the detection of weak, small, cooled regions, such as those associated with the first stages of bubble formation, particularly when other, extended and large amplitude, cooled regions are present For the present analysis we choose α=160, which strikes a balance between the contrasting needs mentioned above.

Apart from measurement noise due to the characteristics of the liquid crystal and of the hue conversion, video noise generated during acquisition and replay can occasionally introduce large amplitude and completely artificial structures in the data arrays. The use of short-time correlations, as described in the following section, allows us to remove some spurious identifications and to locate the position where nucleation events first originate, even when there is no possibility of crosschecking the results with observations on the fluid side.

2.3 Detection and characterization of nucleation events

Various problems affect the performance of the NEF algorithm in locating accurately nucleation events both in time and in space. From the previous work, it is expected that a nucleation event will be preceded by a slow rise in temperature at the site and followed by a rapid fall in temperature over an area approximately matching the size of the bubble, then a slow recovery. The video sampling rate is slow compared to the rate of fall, so there may be only two or three samples during that period, with a sharp transition in temperature, as illustrated in Figure 2. When working on the derived dataset the cooled patch may therefore be first captured when it is small and of low amplitude. This gives the best estimate of the position of the nucleation site at the centre of the patch but the early detection of the patch requires setting the cost function for high sensitivity and can be inhibited by the presence of other strong cooled regions. In the following arrays, the cooled region is of larger amplitude and radius but its centre may not coincide exactly with the nucleation site, e.g. if the bubble grows over a region of initially non-uniform temperature or the bubble is swept sideways by a fluid disturbance. Also background fluctuations and video noise can lead to occasional spurious detection of bubbles by the NEF algorithm, especially when a too high sensitivity of the algorithm was chosen.

In order to obtain a possibly accurate estimate of the nucleation site associated with a nucleation event, the data obtained from the first stage of NEF analysis are postprocessed in order to identify and keep only realistic nucleation events and to trace back the position of cooled areas at the moment of their first formation. To this purpose, at each step in time, the NEFs found are compared with those identified at the previous step: NEFs centred within a certain radius Δr near previous ones are labelled as representing the same nucleation event. For the analysis presented in this paper we used Δr=1 mm. When all NEFs have been assigned to a particular nucleation event, time and position of the first NEF of each sequence are recorded to represent the nucleation site and time. The sampling rate and the ability of the NEF algorithm to detect the appearance of the small and weak cooled region associated with the early stages of bubble formation limit the accuracy in determining the time of initiation of a nucleation event and its initial position.

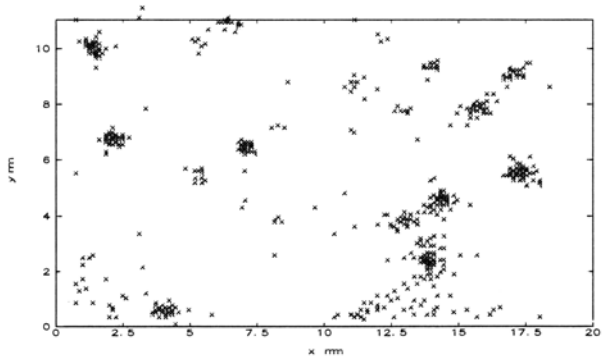

Figure 3: Nucleation sites found by manual analysis (Kenning and Yan 1996) after grouping sites closer than 1 mm.

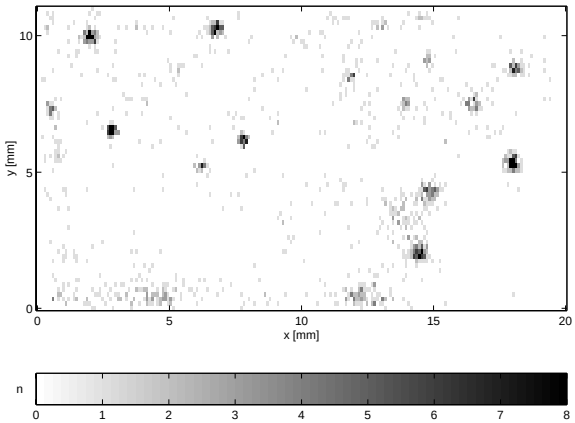

Figure 4: Nucleation sites found by NEF analysis with the parameters indicated in the text, shaded according to number of events at the same site. Darker sites correspond to higher counts.

Once the time and location of a nucleation event have been found, the local wall temperature immediately before nucleation is estimated. In order to reduce the effect of noise, temperature is averaged over a 3x3 cell centred at the nucleation site. This average temperature is followed backward in time from the earliest time of bubble detection and its first maximum is recorded. This allows tracing back to the highest temperature before a drop started, which we define to be the nucleation temperature. Analogously the first minimum temperature following nucleation can be found and assumed to represent the minimum temperature reached by the wall. Occasionally the algorithm identifies spurious nucleation events due to the inaccuracy in the determination of the centre of NEFs with a very large radius. To filter out these events the minimum wall temperature is compared with the nucleation temperature and if the temperature drop is less than 1ºK, the event is discarded.

Comparison of the performance of this algorithm with manual inspection of the sequence of temperature fields, confirms that it is capable of following the evolution in time of individual cooled regions, of discarding spurious nucleation events and of distinguishing the formation of a new bubble at the same site.

The following quantities can be recorded for each nucleation event for statistical analysis: time, position, nucleation temperature, subsequent minimum wall temperature and corresponding radius of the NEF.

3. Results of NEF analysis

3.1 Site positions and nucleation temperatures

The manual analysis at 51 kW/m^2 (Kenning and Yan, 1996) identified more than 600 nucleation events over a period of 12 seconds. Few of these events occurred at positions that coincided exactly, so “nucleation sites” were defined by eliminating small bubbles with lifetimes of less than 20 ms and by consolidating locations lying within 1 mm of each other. This resulted in 552 events at 48 sites, at a low average bubble frequency of 1.15 Hz, shown in Figure 3. The activity at different locations varied enormously. 77% of the bubbles were formed at 12 sites and 20 sites produced only 1 or 2 bubbles during the entire period. The average nucleation superheat and average bubble radius were measured at each site. For a given site, there were only small variations in the nucleation superheat, within the experimental uncertainty of measuring temperature. In a subsequent study of pool boiling of water on a very smooth vertical plate with only a single active site (Wienecke et al. 1999; Kenning et al., 2001), the average activation superheat was 11 K but there was a variation of ± 10% for individual bubbles over 30 s. The temperature gradient in the liquid at the instant of nucleation was estimated from the rate of change of wall temperature and was much too small to explain the variation. These studies raise questions about the conventional model of a nucleation site as a single, micron-sized cavity with a fixed

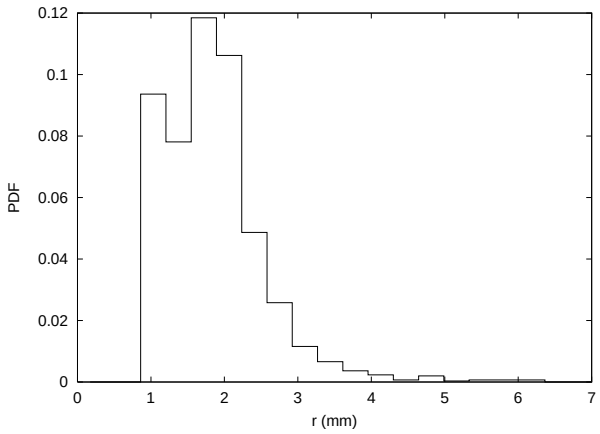

Figure 5: PDF of the radii found by NEF analysis.

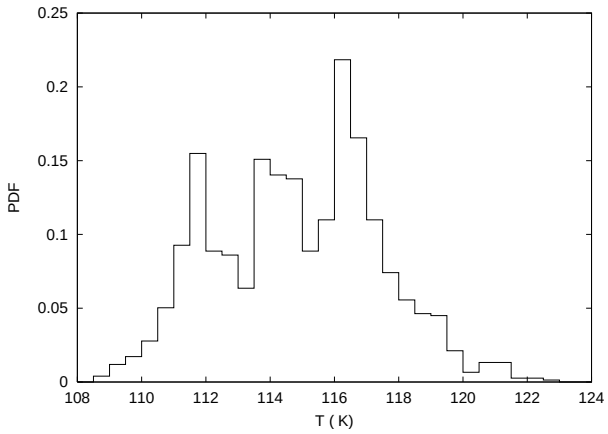

Figure 6: PDF of the nucleation temperatures.

equivalent radius. The effective size of a cavity may not be fixed, or groups of closely-spaced cavities may appear to act as a single site. Further experiments are required analysing data over long periods with high resolution, for which NEF analysis may be a suitable tool.

The automatic NEF analysis of the original data identified 1511 nucleation events, of which 560 during the first 10 seconds. This result is in excellent agreement with the results from the manual analysis and, indeed, manual comparison confirms the accuracy of the identifications. The NEF algorithm identifies 3379 nucleation events, but more than half of them are discarded as spurious or found to correspond to the same event by the postprocessing step. The nucleation events found are shown in Figure 4, where the greyscale shading indicates the number of events at the same site. Comparison with Figure 3 shows that all of the more important clusters of nucleation events found in manual analysis are recovered. Please notice that the origin of coordinates of the field in Figure 4 is offset 0.5 mm to the left with respect to Figure 3. The sites within a cluster are more tightly grouped, which may be a consequence of the improved accuracy of determining the centre of a cooled patch by the automated analysis. The spatial resolution is still not enough to be sure whether or not a cluster really is a group of sites or a single site. Many of the additional sites detected by the NEF analysis produce only one or two small, short-lived bubbles in 30 s, so their contribution to heat transfer would be negligible. The present studies give confidence that nucleation events can be detected from the temperature measurements alone, without the need for simultaneous recording of the bubble side. The consequent simplification in optical arrangements will make it practicable to record the wall temperature patterns at higher resolution.

3.2 Bubble size, frequency and nucleation temperatures

One of the advantages of automatic NEF measurements is the possibility to collect information on physical characteristics of nucleation events such as size, position and nucleation temperature over a large number of events. One possible application of these data is to give a statistical characterisation of nucleation site behaviour for comparisons between data from experiments and numerical simulations. As an example of such statistics, in Figure 5, we plot the probability density function (PDF) of radii of all nucleation events. The increased population in the lowest class ($r=6\ \Delta_y$) is probably due to the fitting of NEFs of this size also to some smaller bubbles ($6\ \Delta_y$ was the smallest radius allowed in the analysis). Please note that the NEF radius is not necessarily the same as the bubble radius. The relationship between NEF radius and the actual bubble size can be obtained by comparison with observations on the fluid side of the plate, but even in absence of this information, such a plot could be used for comparison with other experiments or simulation.

Figure 6 shows the PDF of nucleation temperatures, with three major peaks. The variations in nucleation superheat between events in a cluster is about ± 1°K. The absolute value of the average difference in nucleation

temperatures between events can be fitted to an exponential distribution $p(r)=b\ exp(-a\ T)$, with a = -1.3. This means that 75% of these pairs has a nucleation heat difference smaller than 1°K.

4. Conclusions

It has been shown that fully-computerised NEF analysis can be applied to spatio-temporal data for wall temperature fluctuations in a nucleate boiling system with many nucleation sites. This method makes it possible to develop statistical tools for the comparison of experimental data and numerical simulations. Further work is to be performed to determine the significance of interactions between nucleation sites in extensive systems over long periods.

Acknowledgement: This work was supported by Engineering and Physical Sciences Research Council Grant GR/M89034. T. Kono was on study leave from the Tokyo Electrical Power Company.

References

I. Golobic, E. Pavlovic and S. Strgar, Computer model for nucleation site interactions on a thin plate, Proc. Eurotherm Seminar No. 48, Pool Boiling 2, Paderborn, pp. 33-42, 1996.

Y. He, M. Shoji and S. Maruyama, Numerical study of high heat flux pool boiling heat transfer, Int. J. Heat Mass Transfer, vol. 44, pp. 2357-2373, 2001.

D.B.R. Kenning and Y. Yan, Pool boiling heat transfer on a thin plate: features revealed by liquid crystal thermography, Int. J. Heat Mass Transfer vol. 39, pp. 3117-3137, 1996.

D.B.R. Kenning, T. Kono and M. Wienecke, Investigation of boiling heat transfer by liquid crystal thermography, Experimental Thermal and Fluid Science 25, pp. 219-229, 2001.

P.E. McSharry, L.A. Smith, T. Kono and D.B.R. Kenning, Nonlinear analysis of site interactions in pool nucleate boiling, Proc. 3rd European Thermal Sciences Conference, Heidelberg, vol. 2, pp. 725-730, 2000.

P.E. McSharry, J.H. Ellepola, J. von Hardenberg, L.A. Smith, D.B.R. Kenning and K. Judd, Spatio-temporal analysis of nucleate pool boiling: identification of nucleation sites using non-orthogonal empirical functions, Int. J. Heat Mass Transfer, vol. 45, pp. 237-253, 2001.

K.O. Pasamehmetoglu and R.A. Nelson, Cavity-to-cavity interaction in nucleate boiling: the effect of heat conduction within the heater, AIChE Symposium Series (27th Nat. Heat Transfer Conf., Minneapolis), vol.87, pp. 342-351, 1991.

C. Sadasivan, P. Unal and R.A. Nelson, Nonlinear aspects of high heat flux nucleate boiling heat transfer, Trans. ASME, J. Heat Transfer, vol. 117, pp. 981-988, 1995.

C. Unal and K.O. Pasamehmetoglu, A numerical investigation of the effect of heating methods on saturated nucleate boiling, Int. Comm. Heat Mass Transfer, vol.21, pp. 167-177, 1994.